https://www.cytojournal.com/

CytoJournal

Editor-in-Chief:
Miaoqing Zhao, PhD., MD (Shandong First Medical University, Jinan, China)
He Wang, MD, PhD (Yale University School of Medicine, New Haven, Connecticut, USA)
Founding Editor & Editor-in-chief Emeritus:
Vinod B. Shidham, MD, FIAC, FRCPath (WSU School of Medicine, Detroit, USA)

OPEN ACCESS

Research Article

Sex-determining region Y-Box 4 promotes the progression of advanced hepatocellular carcinoma and enhances regulatory T-cell infiltration and immune suppression

Yingxia Jing[1]*, MM, Yunlong Wu[1], BD

The Intensive Care Unit, The First People's Hospital of Linping District, Hangzhou, China.

***Corresponding author:**

Yingxia Jing,
The Intensive Care Unit, The First People's Hospital of Linping District, Hangzhou, China.

jingyingxia0712@163.com

Received: 11 February 2025
Accepted: 31 March 2025
Published: 02 June 2025

DOI
10.25259/Cytojournal_27_2025

Supplementary material available at:
https: dx.doi.org/10.25259/Cytojournal_27_2025

Quick Response Code:

ABSTRACT

Objective: This study examined the role of sex-determining region Y-box 4 (SOX4) in sorafenib-resistant hepatocellular carcinoma (HCC) cells and its potential therapeutic relevance by focusing on the effects of SOX4 knockdown on tumor growth, apoptosis, and immune infiltration.

Material and Methods: A sorafenib-resistant HCC cell line (sorafenib-resistant HepG2 [SR-HepG2]) was established by gradually increasing the sorafenib dose (1-7 μM) over 12 months. The messenger RNA and protein expression levels of SOX4 in HepG2 and SR-HepG2 cells were analyzed by a quantitative reverse transcription-polymerase chain reaction and Western blot. Small interfering RNA (SOX4) or SOX4 overexpression plasmids were introduced into SR-HepG2 cells through transfection, and the effects on cell proliferation, colony formation, and apoptosis were evaluated using 5-ethynyl-2′-deoxyuridine staining, colony formation assays, and terminal deoxynucleotidyl transferase dUTP nick end labeling assays. For *in vivo* experiments, HepG2 or SR-HepG2 cells were subcutaneously injected into BALB/c nude mice to monitor tumor growth. In the sorafenib-resistant HCC mouse model, SOX4 knockdown (small-interfering RNA SOX4 [si-SOX4]) was delivered through lentiviral vectors to assess its effect on tumor growth. Immune cell infiltration was assessed by immunofluorescence staining, and the influences on immune escape markers were evaluated by Western blot.

Results: Compared with those in the parental HepG2 cells, the transcriptional and translational expression levels of SOX4 were significantly elevated in the SR-HepG2 cells ($P < 0.001$). Si-SOX4 markedly suppressed the proliferation and colony formation of SR-HepG2 cells and increased their cell apoptosis ($P < 0.001$). *In vivo* experiments revealed that si-SOX4 inhibited tumor growth in the sorafenib-resistant HCC model, accompanied by a significant reduction in tumor volume and weight ($P < 0.001$). Histological analysis showed that si-SOX4 disrupted the tumor structure, characterized by increased necrosis and reduced collagen fibers. In addition, si-SOX4 decreased the infiltration of Forkhead box P3+regulatory T cells and cluster of differentiation 11b + myeloid-derived suppressor cells while increasing the number of cluster of differentiation 8 (CD8)+ T cells and granzyme B + CD8+ cytotoxic T cells ($P < 0.001$). SOX4 knockdown also reduced the expression of two immune escape markers, programmed cell death ligand 1 and C-C motif chemokine ligand 12 ($P < 0.001$).

Conclusions: SOX4 overexpression drives sorafenib resistance in HCC cells by promoting cellular growth, inhibiting apoptosis, and enhancing immune evasion. Conversely, SOX4 knockdown inhibits tumor growth, alters immune cell infiltration, and reduces immune escape. Hence, targeting SOX4 is a promising therapeutic approach to overcome sorafenib resistance in HCC.

Keywords: Advanced hepatocellular carcinoma, immune escape, Sex-determining region Y-box transcription factor 4, T cell infiltration

INTRODUCTION

Hepatocellular carcinoma (HCC) continues to be a major contributor to cancer-related mortality worldwide; its occurrence steadily increases, especially in individuals with chronic liver conditions such as cirrhosis and hepatitis.[1,2] In spite of progress in early detection and treatment strategies, the prognosis for advanced HCC remains poor, primarily due to the emergence of treatment resistance.[3,4] Sorafenib, a tyrosine kinase inhibitor with multiple targets, is the standard first-line treatment for advanced HCC and has been shown to extend survival.[5] However, the development of sorafenib resistance remarkably limits its long-term effectiveness and has become one of the major reasons for the high mortality rate in patients with advanced liver cancer.[6]

Recent studies have revealed the complex, multifactorial nature of sorafenib resistance, with increasing evidence indicating that the tumor microenvironment (TME), alterations in intrinsic signaling pathways within tumor cells, and immune evasion mechanisms play critical roles in treatment failure.[7,8] The transcription factor SOX4, a key factor closely associated with resistance in various cancers, belongs to the sex-determining region Y-related HMG-box (SOX) family.[9] It has been recognized as essential in modulating cell proliferation, apoptosis, and immune regulation.[10] The oncogenic and chemotherapy resistance roles of SOX4 in liver cancer have gained increasing attention, but its specific function in sorafenib resistance remains unclear.

This study aims to determine the function of SOX4 in sorafenib resistance in HCC. By establishing a sorafenib-resistant HepG2 (SR-HepG2) cell line and using *in vitro* and *in vivo* models, we aim to uncover the role of SOX4 in the malignant phenotype of liver cancer, particularly in the development of resistance. We hypothesize that SOX4 promotes sorafenib resistance by influencing mechanisms such as cell proliferation, apoptosis, and immune regulation. Therefore, SOX4 could act as a therapeutic target to overcome resistance and improve treatment outcomes for patients with HCC.

This study is important for patients with advanced or severe HCC, as sorafenib resistance significantly hinders effective treatment in these individuals. Understanding the mechanisms by which SOX4 contributes to sorafenib resistance and immune evasion within the TME may provide new insights for therapeutic strategies. In particular, the combination of SOX4 inhibitors with immune checkpoint inhibitors could enhance the effectiveness of current treatment options.

MATERIAL AND METHODS

Cell culture

HepG2 cells (SNL-083) were obtained from SUNNCCELL (Wuhan, China) and cultured using high-glucose Dulbecco's modified eagle medium (DMEM) (iCell-0001, Cellverse Co., Ltd., Shanghai, China) as the basal medium. These cells were authenticated by STR profiling and confirmed to be free of mycoplasma contamination. DMEM was supplemented with 10% fetal bovine serum (iCell-0500, Cellverse Co., Ltd., Shanghai, China) and 1% penicillin-streptomycin (100 U/mL-100 μg/mL) (iCell-15140-122, Cellverse Co., Ltd., Shanghai, China) to prevent bacterial contamination. The cells were incubated at 37°C in a 5% carbon dioxide incubator (CellXpert C170i, Eppendorf, Hamburg, Germany).

Establishment of SR-HepG2 cells

SR-HepG2 cells were established following the method of Xu *et al*.[11] Sorafenib (S7397, Selleck Chemicals, Houston, Texas, USA) with an initial concentration of 1 μM was added to the culture medium of HepG2 cells. Each time the cells adapted to the current dose of sorafenib, the concentration was gradually increased within the range of 1-7 μM. At each sorafenib concentration, the cells were cultured to ensure that they acquired a certain level of resistance and could maintain normal growth, with the entire process lasting 12 months. After 12 months of incremental dosing, the HepG2 cells capable of growing normally in the presence of 7 μM sorafenib were selected and constituted the sorafenib-resistant HCC cell line (SR-HepG2). A drug sensitivity assay was performed on the established SR-HepG2 cells to confirm their resistance to sorafenib, ensuring the successful establishment of the resistant cell line (For more information, please refer to Supplementary Material).

Cell transfection

On the day before transfection, SR-HepG2 cells were seeded into a six-well plate at a 1:1 ratio to ensure 70% confluence at the time of transfection. Add an appropriate amount of small-interfering RNA negative control (Si-NC) (TTCTCCGAACGTGTCACGT) or small-interfering RNA SOX4 (Si-SOX4(1) (CCTTTCTACTTGTCGCTAAAT), Si-SOX4(2) (AGCGACAAGATCCCTTTCATT), Si-SOX4(3) (GAAGAAGGTGAAGCGCGTCTA), overexpression of negative control (Ov-NC), or overexpression of SOX4 (Ov-SOX4) (CAAGCCGGGGGAGAAGG GAGACAAGGTCGGTGGCAGTGGCGGGGGCGGCC ATGGGGGCGGCGGCGGCGGCGGGAGCAGC AACGCGGGG GGAGGAGGCGG CGGTGC GAGTGGCG GCGGCGCCAACTCCAAACCGGCGCAGAAAA AGAGCTGCGGCTCCAAAGTGGCGGGCGGC GCGGGCGGTGGGGTTAGCAAACCGCACGCCA AGCTCATCCTGGCAGGCGGCGGCGGCGGC GGGAAAGCAGCGGCTGCCGCCGCCGCCTCCT TCGCCGCCGAACAGGCGGGGGCCGCCGCCCTG CTGCCCCTGGGCGCCGCCGCCGACCACCAC TCGCTGTACAAGGCGCGGACTCCCAGCGCC

TCGGCCTCCGCCTCCTCGGCAGCCTCGGCCTCCGCAGCGCTCGCGGCCCCGGGCAAGCACCTGGCGGAGAAGAAGGTGAAGCGCGTCTACCTGTT) plasmid to a serum-free medium, and add Lipofectamine 3000 (L3000008, Invitrogen, Carlsbad, California, USA) to the serum-free medium, mixing gently. Let it stand for 5 min, then mix the plasmid and transfection reagent, incubating at room temperature for 15 min to form the plasmid-transfection reagent complex. The plasmid-transfection reagent complex was added to the cell culture dish and mixed gently. Culturing was continued for 48 h, and the transfection efficiency was verified.

Animal experiment

Forty male BALB/c nude mice (4-6-weeks-old, weighing 20-25 g) were purchased from BesTest Biotechnology Co., Ltd. (Zhuhai, China) and housed in an environment with a temperature of 20-25°C, humidity between 40% and 60%, and a light cycle consisting of 12 h of light and 12 h of darkness. The animal experiment design and execution in this study were adapted from the research of Xu *et al.*[11] Ten BALB/c nude mice were randomly selected as the Model group, and HepG2 cells (1×10^6 cells/100 μL of phosphate-buffered saline [PBS]) were subcutaneously injected into their back area. The remaining 30 mice were used to establish the SR-Model group, and SR-HepG2 cells (at the same concentration) were subcutaneously injected into their dorsal region. After injection, the tumors in the Model and SR-Model groups were allowed to grow *in vivo* for 4 weeks, during which tumor growth was regularly monitored. After 4 weeks, 10 mice from the SR-Model group and 10 mice from the Model group were euthanized to collect tumor tissues. The remaining 20 SR-Model mice were randomly divided into SR-si-NC or SR-si-SOX4 groups where si-NC or si-SOX4 lentiviral vectors (SinaBiological, LVCV-01, Beijing, China) were injected, respectively. Si-NC or si-SOX4 lentiviral vectors were directly injected into the tumor site 3 times a week for 2 weeks. After the treatment, the mice were observed for an additional 2 weeks and euthanized through an intraperitoneal injection of 3% pentobarbital sodium (57-33-0, Merck, Darmstadt, Germany) (110 mg/kg). This study was approved by the Beijing Maide Kangna Laboratory Animal Welfare Ethics Committee (approval no. MDKN-2025-006).

Quantitative reverse transcription-polymerase chain reaction (qRT-PCR)

Total RNA was isolated using the TRIzol reagent (R0016, Beyotime, Shanghai, China). RNA purity was measured using a spectrophotometer (ultraviolet-2600, Shimadzu, Kyoto, Japan). The extracted RNA was reverse transcribed into complementary DNA (cDNA) using a reverse transcription kit (D7170S, Beyotime, Shanghai, China) following the manufacturer's instructions. The cDNA, specific primers, and SYBR Green were mixed and added to qRT-PCR reaction tubes. Cycling amplification was performed using a real-time PCR machine (LightCycler 96, Roche, Basel, Switzerland). The relative expression levels of the target gene were calculated using cycle threshold values, with glyceraldehyde-3-phosphate dehydrogenase (GAPDH) as the internal control for normalization ($2^{-\Delta\Delta Ct}$ method). The primer sequences utilized in this study are provided in Table 1.

Western blot

Total protein was isolated using a lysis buffer (P0013B, Beyotime, Shanghai, China). Protein concentrations were measured using the BCA assay (P0009, Beyotime, Shanghai, China). The protein samples were combined with a loading buffer and separated through Sodium Dodecyl Sulfate-Polyacrylamide Gel Electrophoresis. Following separation, the proteins were transferred onto a polyvinylidene fluoride membrane (FFP19, Beyotime, Shanghai, China). To block non-specific binding, the membrane was treated with 5% bovine serum albumin (BSA) (P0007, Beyotime, Shanghai, China). Subsequently, the membrane was incubated with primary antibodies (SOX4 (1:1000, ab316850), programmed death-ligand 1 (PD-L1) (1:1000, ab205921), C-C motif chemokine ligand 12 (CCL12) (1:1000, ab9737), GAPDH (1:1000, ab8245) and secondary antibodies (1:1000, ab6728, ab6721), followed by washing to remove unbound antibodies. Signal detection was performed using an enhanced chemiluminescent substrate (ECL) (P0018S, Beyotime, Shanghai, China), and protein bands were captured using a gel imaging system (ChemiDoc XRS+, Bio-Rad, Hercules, California, USA). Protein expression levels were measured using ImageJ software (version 1.5f, National Institutes of Health [NIH], Bethesda, Maryland, USA). The antibodies were sourced from Abcam, Cambridge, UK.

Table 1: Primer sequences.

Primes name	Primes sequences
Hum-SOX4-F	CCCAGCAAGAAGGCGAGTTA
Hum-SOX4-R	CCTTCCAGTTCGTGTCCTCC
Hum-GAPDH-F	GTGGATATTGTTGCCATCAATGACC
Hum-GAPDH-R	GCCCCAGCCTTCTTCATGGTGGT
Mus-SOX4-F	AGGACAGCGACAAGATTCCG
Mus-SOX4-R	TGCCCGACTTCACCTTCTTTC
Mus-GAPDH-F	TGTCTCCTGCGACTTCAACA
Mus-GAPDH-R	GGTGGTCCAGGGTTTCTTACT

Hum: Human, SOX4: SRY-box transcription factor 4, Mus: Mouse, GAPDH: Glyceraldehyde-3-phosphate dehydrogenase, F: Forward; R: Reverse, A: Adenine, C: Cytosine, G: Guanine, T: Thymine

Cell colony formation assay

First, the cells in the logarithmic growth phase were digested, counted, and seeded into a six-well plate at a density of approximately 1000 cells/well. An appropriate culture medium was added, and the cells were incubated for 7 days until visible colonies had formed. The cells were fixed for 15 min, followed by staining with crystal violet solution (C0121, Beyotime, Shanghai, China) for 10 min. The cells were gently washed with water to remove excess dye. Finally, the colonies formed in each well were observed and counted under a microscope (AE31, Motic, Beijing, China).

5-Ethynyl-2′-deoxyuridine (EdU) staining

Cells (1×10^5 cells/well) were seeded into a six-well plate, and staining was performed when the confluence reached 70-80%. In accordance with the EdU kit (C0071S, Beyotime, Shanghai, China) instructions, the EdU solution was added to the culture medium, and the cells were incubated for 4 h. After fixation and permeabilization, the EdU staining reagent was added (as per the kit instructions) to the cells and incubated for 30 min. A 4′,6-diamidino-2-phenylindole (DAPI) solution was added to stain the cell nuclei, and incubation was continued for another 5 min. The EdU-labeled cells were observed under a fluorescence microscope (EVOS FL, Thermo Fisher Scientific, Waltham, Massachusetts, USA). Positive cells were quantified using ImageJ software (version 1,5f, NIH, Bethesda, Maryland, USA).

Terminal deoxynucleotidyl transferase dUTP nick end labeling (TUNEL) staining

Cells (1×10^5 cells/well) were seeded into a six-well plate, fixed, and permeabilized when the confluence reached 70-80%. The TUNEL reaction solution was prepared in accordance with the TUNEL kit (C1086, Beyotime, Shanghai, China) instructions and added to the cells, followed by incubation at 25°C for 60 min. A DAPI solution was added to stain the cell nuclei, and incubation was performed for another 5 min. The staining results were observed under a fluorescence microscope (EVOS FL, Thermo Fisher Scientific, Waltham, Massachusetts, USA). Positive cells were quantified using ImageJ software (version 1,5f, NIH, Bethesda, Maryland, USA).

Hematoxylin and eosin (HE) staining

First, fix the tumor tissue and process it through dehydration, clearing, and paraffin embedding. The tissue was into 4-5 μm-thick sections, which were deparaffinized in xylene and gradually hydrated with different alcohol concentrations. HE staining was performed by immersing the sections in hematoxylin (C0105S, Beyotime, Shanghai, China) stain for 5 min, washing with water, and differentiating the sections with 1% hydrochloric acid alcohol solution, followed by water washing. The sections were immersed in eosin stain for 5 min, washed with water, and dehydrated. Finally, the sections were serially dehydrated with alcohol (70%, 95%, and 100%), cleared in xylene, and mounted on slides. After completion, the morphological changes in the tissue sections were observed and analyzed using a microscope (AE31, Motic, Beijing, China).

Masson staining

First, fix the tissue specimen and process it through dehydration, clearing, and paraffin embedding. The tissue was then cut into 4-5 μm-thick sections. These sections were deparaffinized and gradually hydrated with different alcohol concentrations (100%, 95%, and 70%). After that, perform the staining: immerse the sections in phosphomolybdic acid (Y000614, Beyotime, Shanghai, China) solution for 10 min, then wash with water; next, immerse the sections in hematoxylin stain for 5 min, followed by water washing; then, immerse the sections in acidic ponceau stain for 5 min, and wash with water; finally, immerse the sections in acidic ponceau-transparent solution for 5 min, then wash clean. Afterward, the sections were serially dehydrated with alcohol (70%, 95%, and 100%), cleared in xylene, and mounted on slides. After Masson staining (C0189S, Beyotime, Shanghai, China), collagen fibers will appear blue or green, cell nuclei will appear blue, and muscle and red blood cells will appear red. The stained sections were observed and analyzed under a microscope (AE31, Motic, Beijing, China).

Immunofluorescence staining

Immune cell markers were detected following the method of Luo *et al.*[12] First, fix the tumor tissue, followed by dehydration, clearing, and paraffin embedding. The tissue was cut into 4-5 μm-thick sections and transferred to glass slides, allowing them to adhere. The sections were then deparaffinized and rehydrated. Antigen retrieval was performed. Non-specific binding was blocked by incubating the sections with 5% BSA at room temperature for 1 hour. The diluted primary antibodies (Forkhead box P3 [Foxp3] (1:500, ab243890), F4/80 (1:500, ab6640), cluster of differentiation 11b (CD11b) (1:500, ab52478), cluster of differentiation 8 (CD8) (1:500, ab237709), and Granzyme B (GZMB) (1:500, ab243879)) were added, and the sections were incubated overnight at 4°C. The sections were washed three times with PBS for 5 min each to remove unbound primary antibodies. Fluorescently labeled secondary antibodies (Alexa Fluor 594) (1:1000, ab150120, ab150080) were then added, followed by incubation at room temperature for 1 hour. Cell nuclei were stained with DAPI (C1002, Beyotime, Shanghai, China)

for 5 min, and the sections were finally mounted with an anti-fade reagent. The fluorescence signals in the sections were observed using a fluorescence microscope (EVOS FL, Thermo Fisher Scientific, Waltham, Massachusetts, USA). The distribution and expression of Foxp3, F4/80, CD11b, CD8, and GZMB-positive cells were analyzed, and quantitative analysis was performed using ImageJ software (version 1,5f, NIH, Bethesda, Maryland, USA). The antibodies were sourced from Abcam, Cambridge, UK.

Statistical analysis

Data were analyzed using GraphPad Prism software (version 9.0, GraphPad Software, San Diego, California, USA), and the results were presented as mean ± standard deviation. T-test was used for comparisons between two groups, and a one-way analysis of variance was used for comparisons among multiple groups, followed by Tukey's *post hoc* test. A $P < 0.05$ was considered statistically significant.

RESULTS

SOX4 overexpression in SR-HCC cells

First, we established an SR-HCC cell line (SR-HepG2) by gradually increasing the sorafenib dose (1-7 μM) administered to HepG2 cells for 12 months. Next, we measured SOX4 expression in HepG2 and SR-HepG2 cells. Figure 1a-c shows that the messenger RNA (mRNA) and protein levels of SOX4 were markedly elevated in SR-HepG2 cells compared with those in HepG2 cells ($P < 0.001$).

SOX4 knockdown inhibits growth of SR-HepG2 cells

Next, we transfected small interfering RNA (siRNA) (SOX4) and SOX4 overexpression plasmids into SR-HepG2 cells. Figures 2a and b show that siRNA (SOX4) and SOX4 overexpression plasmid successfully knocked down or overexpressed the SOX4 gene in SR-HepG2 cells ($P < 0.01$). We then selected the most efficient siRNA (SOX4) and SOX4 overexpression plasmids for subsequent experiments. Si-NC and Ov-NC had no effect on SOX4 expression. Colony formation assays [Figure 2c and d] revealed that the number of colonies formed by SR-HepG2 cells was significantly reduced by si-SOX4 and significantly increased by Ov-SOX4 ($P < 0.001$). Figures 2e and f show that compared with those in the si-NC group, the number of EdU-positive cells in SR-HepG2 cells was notably reduced by si-SOX4 and significantly increased by Ov-SOX4 ($P < 0.001$). Figures 2g and h indicate that si-SOX4 notably increased the number of apoptotic cells in SR-HepG2 cells, whereas Ov-SOX4 significantly decreased the number of apoptotic cells ($P < 0.001$).

Si-SOX4 inhibits the growth of sorafenib-resistant HCC tumors

To further validate the role of SOX4 in mediating sorafenib resistance in HCC *in vivo*, we subcutaneously injected HepG2 cells (Model group) and SR-HepG2 cells (SR-Model group) into BALB/c nude mice and allowed them to grow for 4 weeks. Tumor tissues were then collected to assess SOX4 expression. Figure 3a-c shows that compared with the Model group, the SR-Model group exhibited significantly increased SOX4 mRNA and protein levels in tumor tissues ($P < 0.01$, $P < 0.001$). Next, we treated the SR-Model mice with sorafenib for 4 weeks. In parallel, si-NC or si-SOX4 lentiviral vectors were injected into the tumor sites for 2 weeks [Figure 3d]. Consistent with the *in vitro* results, si-SOX4 treatment significantly reduced the mRNA and protein expression levels of SOX4 in the HCC tumor tissues ($P < 0.01$, $P < 0.001$) [Figures 3e-g]. Figure 3h-j shows that si-SOX4 treatment significantly inhibited tumor growth, with a notable reduction in tumor weight and volume ($P < 0.001$).

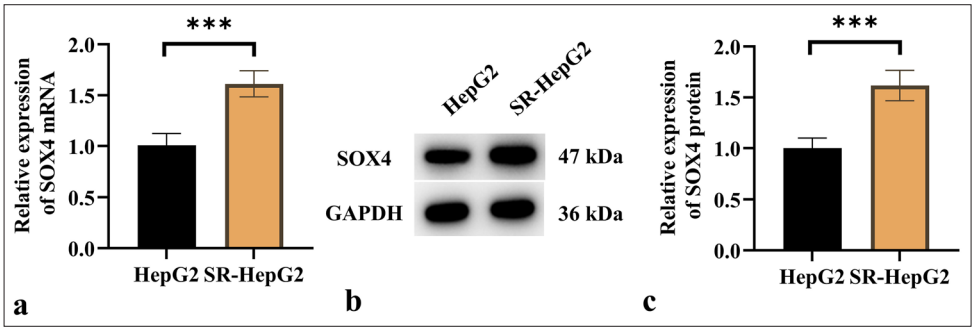

Figure 1: SOX4 overexpression in SR-HCC Cells. (a) messenger RNA levels of SOX4 in HepG2 parental cells and SR-HepG2. (b and c) Protein levels of SOX4 in HepG2 cells and SR-HepG2 cells. $n = 6$. ***$P < 0.001$. SOX4: SRY-box transcription factor 4, GAPDH: Glyceraldehyde-3-phosphate dehydrogenase, SR-HCC: Sorafenib-resistant hepatocellular carcinoma, SR-HepG2: Sorafenib-resistant HepG2.

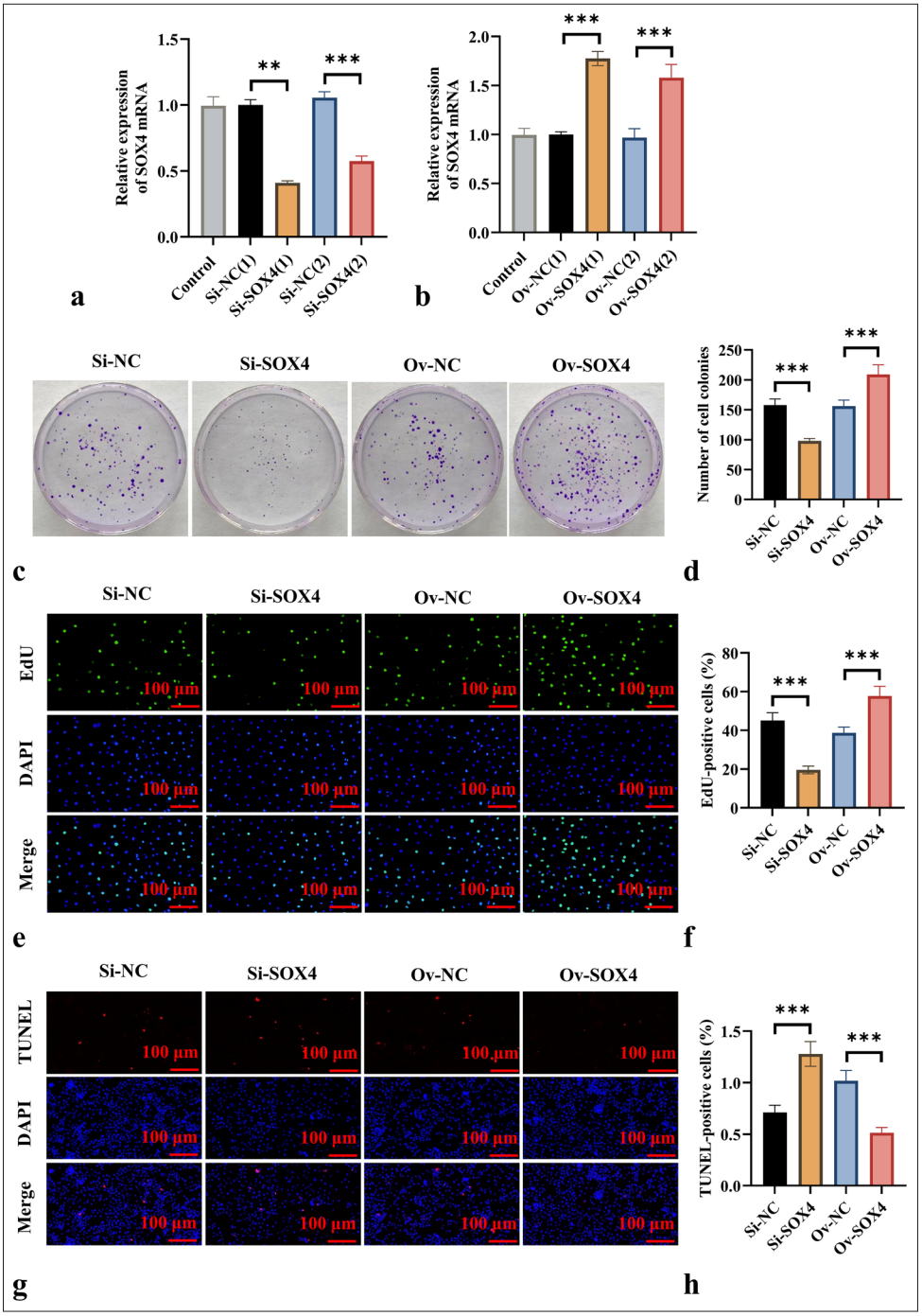

Figure 2: SOX4 knockdown inhibits the growth of SR-HepG2 cells. (a and b) qRT-PCR analysis to verify the transfection efficiency of SOX4 knockdown or overexpression in SR-HepG2 cells. (c and d) Effect of SOX4 knockdown or overexpression on the colony formation of SR-HepG2 cells. (e and f) Effect of SOX4 knockdown or overexpression on the proliferation of SR-HepG2 cells. Magnification ×200. Scale bar: 100 μm. (g and h) Effect of SOX4 knockdown or overexpression on the apoptosis of SR-HepG2 cells. Magnification ×200. Scale bar: 100 μm. $n = 6$. $^{**}P < 0.01$, $^{***}P < 0.001$. Si-NC: Small-interfering RNA negative control, Si-SOX4: Small-interfering RNA SOX4, Ov-NC: Overexpression of negative control, Ov-SOX4: Overexpression of SOX4, EdU: 5-Ethynyl-2′-deoxyuridine, DAPI: 4′,6-Diamidino-2-phenylindole, TUNEL: Terminal deoxynucleotidyl transferase dUTP nick end labeling, qRT-PCR: Quantitative reverse transcription-polymerase chain reaction, SR-HepG2: Sorafenib-resistant HepG2.

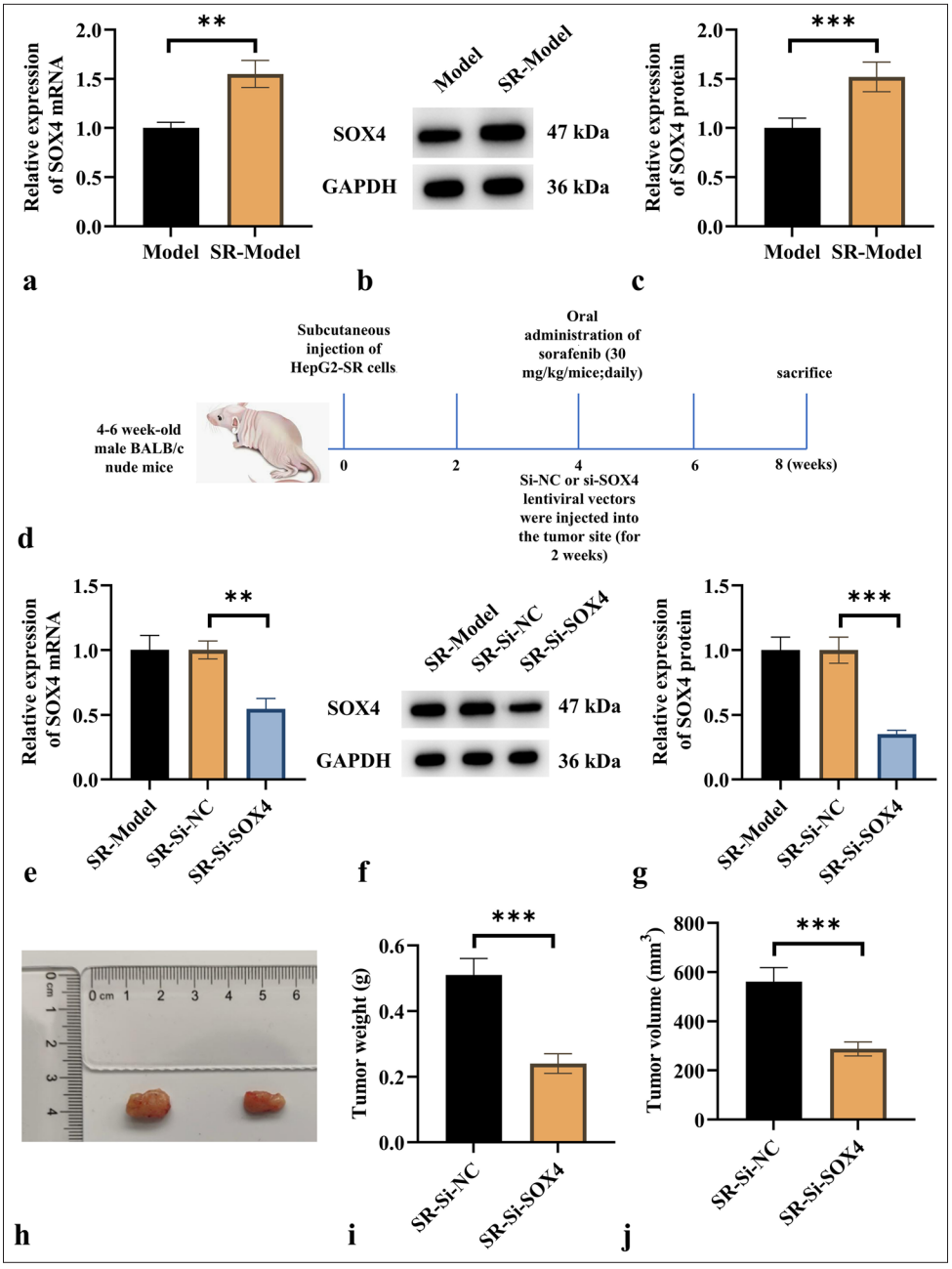

Figure 3: Si-SOX4 inhibits the growth of sorafenib-resistant HCC tumors. (a) Subcutaneous injection of HepG2 cells (Model group) and SR-HepG2 cells (SR-Model group) into BALB/c nude mice and tumor growth for 4 weeks. SOX4 mRNA levels were measured in tumor tissues from the Model and SR-Model groups. (b and c) Measurement of SOX4 protein levels in tumor tissues from the Model and SR-Model groups. (d) Experimental design for the establishment of the HCC model in SR-Model mice and subsequent treatment (Graphics Suite 2022, CorelDRAW, Corel Corporation). (e) Effect of different treatments on SOX4 mRNA expression in sorafenib-resistant HCC tumors. (f and g) Effect of different treatments on SOX4 protein expression in sorafenib-resistant HCC tumors. (h) Representative images of tumors under different treatments. (i and j) Effect of different treatments on tumor weight and volume. $n = 10$. ** $P < 0.01$, ***$P < 0.001$. Si-SOX4: Small-interfering RNA SOX4, mRNA: Messenger RNA, HCC: Hepatocellular carcinoma, SR-HepG2: Sorafenib-resistant HepG2, GAPDH: Glyceraldehyde-3-phosphate dehydrogenase, BALB/c mice: Bagg albino mice.

We also performed histological analysis of the tumor tissues using HE staining. In the SR-si-NC group, the tumor cells showed high heterogeneity, intact cellular structures, regular cell arrangement, increased nuclear atypia, and distinct mitotic figures. By contrast, the tumor tissues in the SR-si-SOX4 group showed disrupted structures with focal necrosis, disorganized cell arrangement, and reduced mitotic figures [Figure 4a]. Masson staining results revealed that compared with the SR-si-NC group, the SR-si-SOX4 group exhibited a significant reduction in blue collagen fibers, thinning of blood vessel walls, reduced fibrosis, and increased levels of inflammatory infiltration [Figure 4b].

Si-SOX4 inhibits Treg cell infiltration in HCC mouse tumors

We further investigated the regulatory effect of si-SOX4 on the immune microenvironment in HCC. Figure 5a-j demonstrates that si-SOX4 treatment significantly reduced the infiltration of Foxp3+ Tregs ($P < 0.001$), decreased the infiltration of CD11b+ MDSC cells ($P < 0.001$), significantly increased the infiltration of CD8+ T cells ($P < 0.001$), and increased the infiltration of granzyme B-positive (GZMB+) CD8+ cytotoxic T cells ($P < 0.05$). No significant difference in the proportion of F4/80+ cells was observed between the groups. These findings suggest that SOX4 primarily affects the abundance of Tregs, MDSCs, and CD8+ T cells within HCC tumors.

Si-SOX4 inhibits immune evasion in HCC mice

We measured the protein expression levels of PD-L1 and CCL12 in tumor tissues. Figure 6a-c shows that the protein expression levels of PD-L1 and CCL12 were significantly reduced in the SR-si-SOX4 group compared with those in the SR-si-NC group ($P < 0.001$).

DISCUSSION

In this study, we successfully established an SR-HCC cell line (SR-HepG2) by gradually increasing the concentration of sorafenib (HepG2 cells exposed to 1-7 μM sorafenib) and demonstrated the critical role of SOX4 in promoting sorafenib resistance. By comparing SR-HepG2 cells with their parent HepG2 cells, we found that SOX4 was notably upregulated in the resistant cells. This SOX4 upregulation was a key event, as our subsequent experiments showed that SOX4 knockdown suppressed the growth of SR-HepG2 cells, but its overexpression enhanced cell proliferation and reduced apoptosis. These findings suggest that SOX4 plays a potential driving role in the malignant phenotype of SR-HCC and may act as a promoter of resistance mechanisms.

These findings have significant clinical implications in the context of severe HCC. With the worsening of HCC malignancy, especially in patients with advanced or resistant HCC, sorafenib, a standard treatment, has become one of the major causes of treatment failure due to resistance.[13] Our results suggest that SOX4 plays a crucial role in sorafenib resistance by promoting tumor cell proliferation and inhibiting apoptosis. Therefore, SOX4 is a potential driver of resistance mechanisms and a possible therapeutic target for overcoming HCC resistance.

Consistent with the growing body of research, SOX4 plays a vital role in cancer progression, chemotherapy resistance, and immune escape.[14,15] As a transcription factor of the SOX family, SOX4 has been shown to be involved in various oncogenic processes, including chemotherapy resistance.[16,17]

In addition to its role in promoting proliferation, SOX4 further enhanced sorafenib resistance by inhibiting apoptosis. Our TUNEL assay results show that silencing SOX4 significantly increased apoptosis in SR-HepG2 cells, and overexpressing it produced the opposite effect. This finding is consistent with previous studies, which suggest that SOX4 inhibits apoptosis in various cancers by regulating key apoptotic pathways, such as downregulating pro-apoptotic factors and upregulating anti-apoptotic proteins, thereby promoting cancer cell survival under cytotoxic drug exposure.[18,19] In this study, SOX4 may confer sorafenib resistance by inhibiting apoptosis, allowing cancer cells to evade the cytotoxic effects of the drug.

By establishing a xenograft model using nude mice, we validated the role of SOX4 in sorafenib resistance. We found that SOX4 expression was significantly higher in the tumors derived from SR-HepG2 cells than in those derived from HepG2 cells. Silencing SOX4 reduced its expression and significantly inhibited tumor growth, as evidenced by a decrease in tumor volume and weight. These results suggest that targeting SOX4 may be an effective strategy to overcome sorafenib resistance in HCC. Furthermore, pathological analysis of the tumor tissue revealed that inhibition of SOX4 disrupted tumor structure, increased tumor necrosis, and reduced fibrosis, indicating that SOX4 may promote resistance by affecting tumor cell behavior and altering the TME.

Another significant discovery of this study is the regulatory role of SOX4 in the immune microenvironment of HCC. TME plays a crucial role in cancer progression and treatment resistance.[20] Immunosuppressive cells, such as Tregs and MDSCs, contribute to tumor survival by promoting immune suppression.[21,22] We found that silencing SOX4 in SR-HepG2 tumors significantly reduced the infiltration of Foxp3+ Tregs and CD11b+ MDSCs and increased the infiltration of CD8+ cytotoxic T cells. This change is critical, as Tregs and MDSCs are known to suppress anti-tumor immune responses, and CD8+ T cells play a vital role in tumor killing. We also observed an increase in GZMB+ CD8+ cells in the SOX4

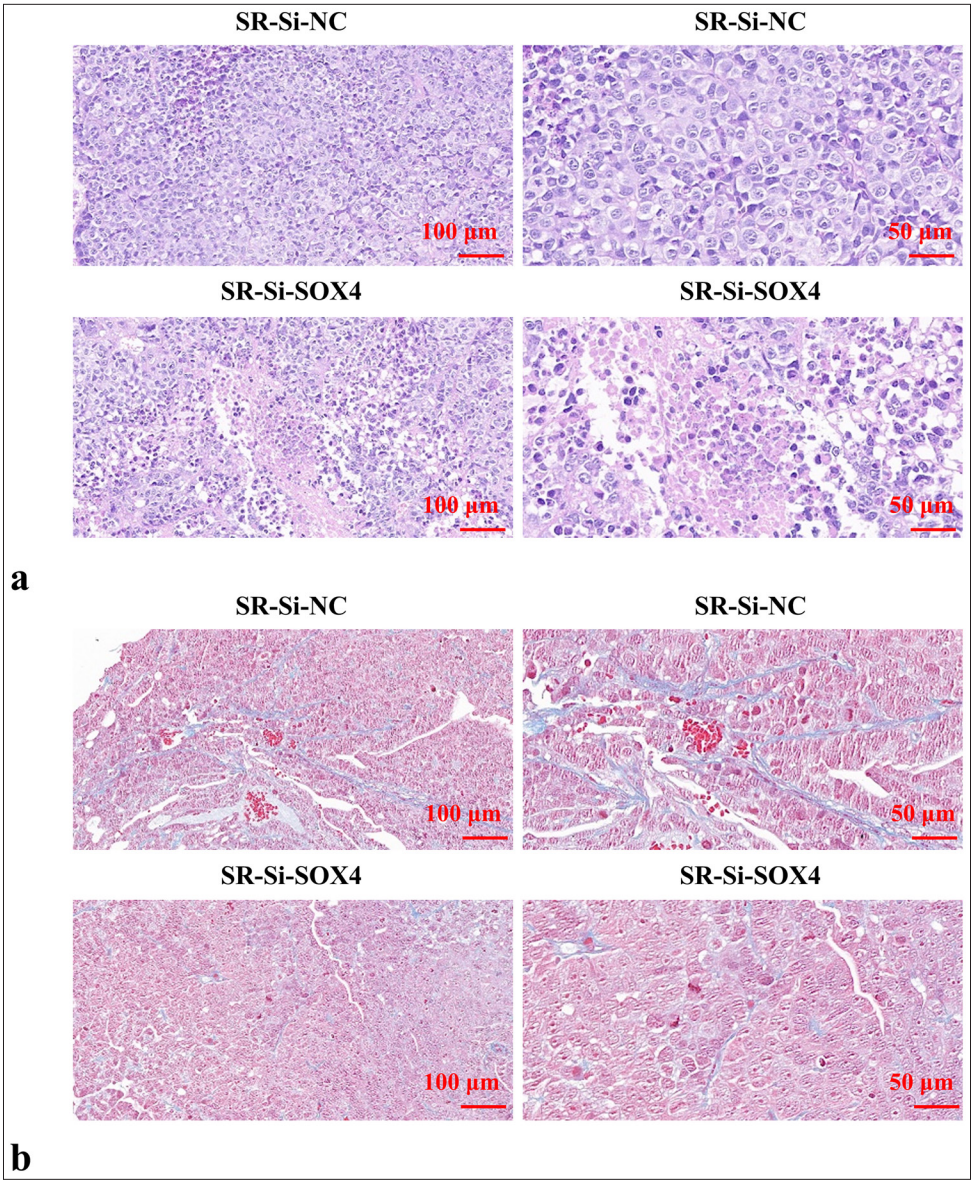

Figure 4: Si-SOX4 treatment disrupts tumor tissue structure. (a) HE staining analysis of tumor tissues after different treatments. Magnification ×200 and ×400. Scale bar: 100 and 50 μm. (b) Masson staining analysis of tumor tissues after different treatments. Magnification ×200 and ×400. Scale bar: 100 and 50 μm. n = 10. Si-SOX4: Small-interfering RNA SOX4, HE: Hematoxylin and eosin.

knockdown group, further confirming that SOX4 enhances T cell cytotoxic activity and improves anti-tumor immune responses.

The immunoregulatory role of SOX4 is important in sorafenib resistance. Sorafenib exerts its effects on tumor cells through direct anti-proliferative action and influences immune responses by modulating the TME.[23,24] However, the development of sorafenib resistance may be associated with changes in the TME that favor tumor growth.[25] Our study suggests that SOX4 may be a key regulator of immune evasion mechanisms, as silencing SOX4 reduced the expression of PD-L1 and CCL12 in sorafenib-resistant tumors. PD-L1 is an immune checkpoint molecule, and its upregulation inhibits T-cell activity and thus promotes immune evasion. Suppressing SOX4 reduced PD-L1 expression, indicating that targeting SOX4 may enhance the efficacy of PD-1/PD-L1 immune checkpoint inhibitors by alleviating immune suppression.

CCL12 is a chemokine that is involved in the recruitment of MDSCs and promotes immune suppression and tumor

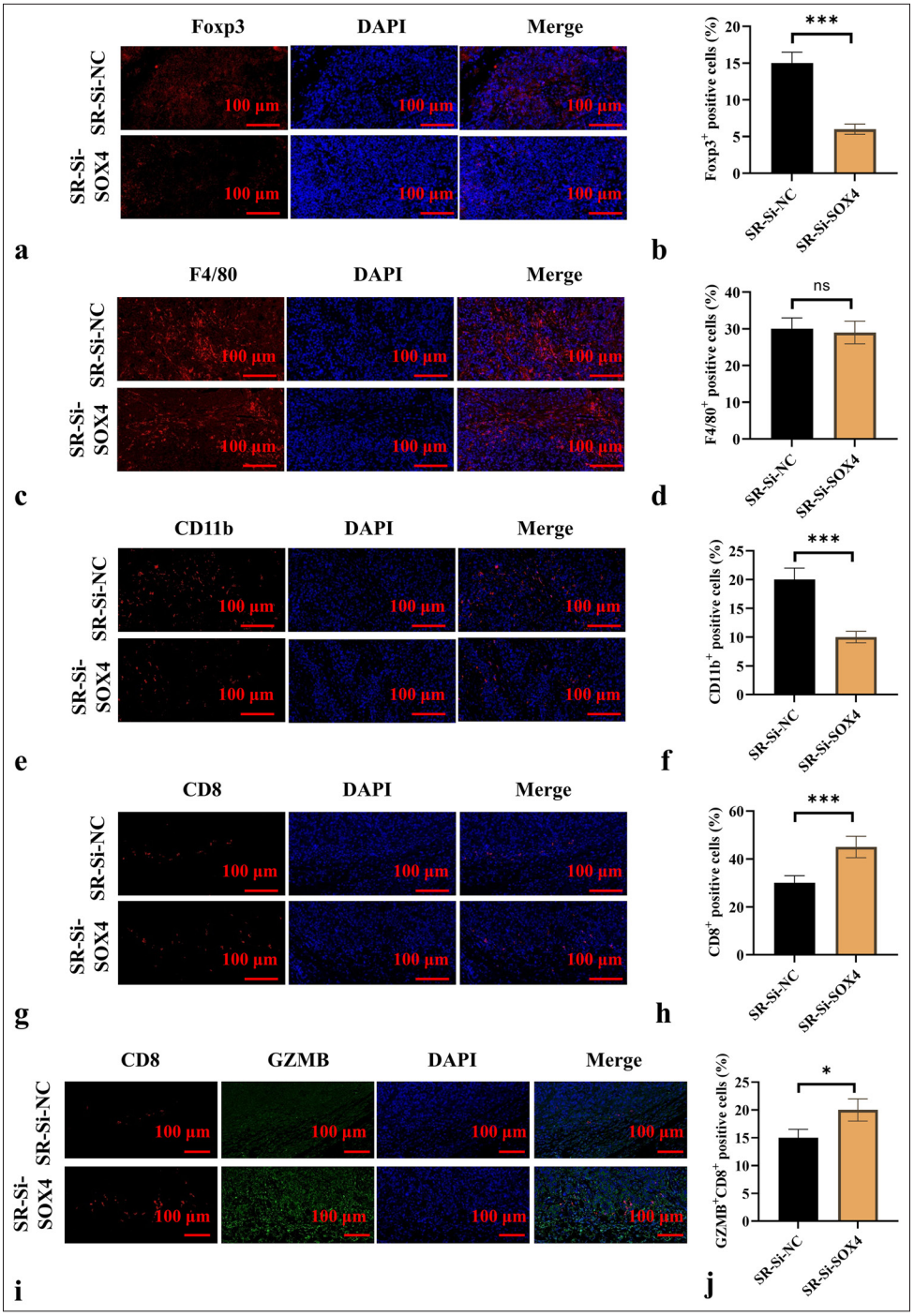

Figure 5: Si-SOX4 inhibits treg cell infiltration in HCC mouse tumors. (a and b) Immunofluorescence (IF) staining measuring the levels of Foxp3+ cells in tumor tissues. Magnification ×200. Scale bar: 100 μm. (c and d) IF staining measuring the levels of F4/80+ cells in tumor tissues. Magnification 200x. Scale bar: 100 μm. (e and f) IF staining measuring the expression levels of CD11b+ cells in tumor tissues. Magnification ×200. Scale bar: 100 μm. (g and h) IF staining measuring the expression levels of CD8+ cells in tumor tissues. Magnification ×200. Scale bar: 100 μm. (i and j) IF staining measuring the expression levels of GZMB+ CD8+ cells in tumor tissues. Magnification ×200. Scale bar: 100 μm. $n = 10$, ns: No significant difference; *$P < 0.05$, ***$P < 0.001$. Foxp3: Forkhead box P3, F4/80: F4/80 antigen, CD11b: Cluster of differentiation 11b, CD8: Cluster of differentiation 8, GZMB: Granzyme B, SOX4: SRY-box transcription factor 4, DAPI: 4′,6-Diamidino-2-phenylindole.

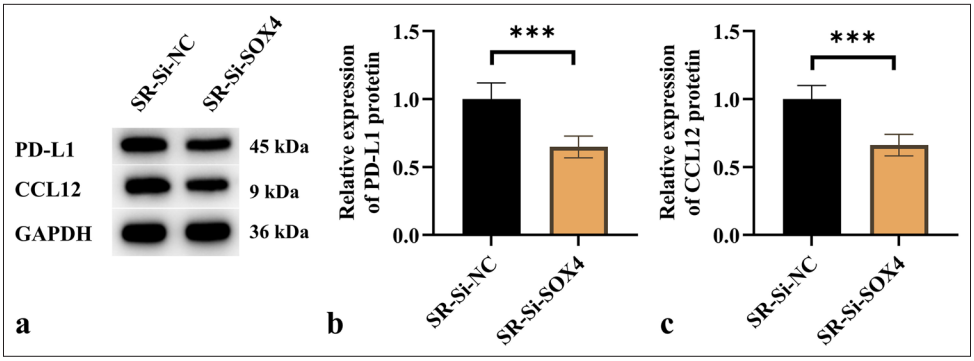

Figure 6: Si-SOX4 inhibits immune evasion in HCC mice. (a-c) Western blot analysis of PD-L1 and CCL12 protein expression levels in tumor tissues. $n = 10$, ***$P < 0.001$. Si-SOX4: Small-interfering RNA SOX4, PD-L1: Programmed cell death ligand 1, CCL12: C-C motif chemokine ligand 12, HCC: Hepatocellular carcinoma, GAPDH: Glyceraldehyde-3-phosphate dehydrogenase.

growth.[26,27] Silencing SOX4 reduced CCL12 expression, highlighting the role of SOX4 in regulating the TME. By reducing MDSC recruitment, SOX4 inhibition may help restore the immune system's effective anti-tumor response.

This study mainly relied on *in vitro* experiments to assess the effects of SOX4 knockdown on the proliferation and apoptosis of SR-HepG2 cells. Although cell line models provide convenience for research, they do not fully replicate the complexity of the TME *in vivo*. Therefore, the applicability and effectiveness of the experimental results in clinical settings, particularly in patients with HCC, require further validation. In addition, this study only used the HepG2 cell line and its sorafenib-resistant derivative, SR-HepG2, to investigate the role of SOX4. However, different HCC cell lines may exhibit distinct molecular characteristics and resistance mechanisms. The use of a single cell line may limit the generalizability of the findings. Future studies should include multiple HCC cell lines to validate the role of SOX4 across diverse HCC contexts and ensure the reproducibility and clinical relevance of the results. In the *in vivo* experiments, BALB/c nude mice were used as a tumor model. However, these immunodeficient mice cannot fully mimic the complexity of the human immune system, especially in studies of tumor immune infiltration and immune evasion. Therefore, the observed effects of SOX4 knockdown on the tumor immune microenvironment may not be directly translatable to clinical practice. Future research should employ animal models with fully functional immune systems to better simulate the immune responses of human HCC. Although this study demonstrated that SOX4 promotes sorafenib resistance in HCC, resistance mechanisms in HCC are often driven by multiple factors and potentially involve other signaling pathways and genes. Studying the role of SOX4 alone may not fully elucidate all the mechanisms of resistance in HCC. Future studies should consider incorporating other resistance-related genes and pathways for a comprehensive analysis. Although this study suggests that SOX4 knockdown could be a potential therapeutic strategy to overcome sorafenib resistance, the findings remain at a preclinical stage. Extensive clinical trials are warranted to evaluate the safety, efficacy, and tolerability of SOX4 inhibition in patients. Furthermore, the development and clinical application of SOX4 inhibitors face technical and economic challenges.

In summary, our study identifies SOX4 as a critical factor in mediating sorafenib resistance in HCC. SOX4 contributes to the development of resistance through several mechanisms, including promoting tumor cell proliferation, inhibiting apoptosis, and influencing the tumor immune microenvironment. Therefore, targeting SOX4 offers a promising approach to overcoming sorafenib resistance, addressing the intrinsic resistance mechanisms of the tumor, and enhancing anti-tumor immune responses. Future studies should investigate the molecular pathways downstream of SOX4 and its role in these processes and assess the potential of combining SOX4 inhibition with immune therapies or other targeted treatments to provide novel strategies for improving the therapeutic outcomes of patients with HCC.

SUMMARY

This study demonstrates that SOX4 promotes sorafenib resistance in HCC by enhancing tumor cell proliferation, inhibiting apoptosis, and modulating the immune microenvironment. Hence, targeting SOX4 could be a promising strategy to overcome sorafenib resistance and improve treatment outcomes.

AVAILABILITY OF DATA AND MATERIALS

The data that support the findings of this study are available from the corresponding author upon reasonable request.

ABBREVIATIONS

A: Adenine
C: Cytosine
CCL12: C-C motif chemokine ligand 12
CD11b: Cluster of differentiation 11b
CD8: Cluster of differentiation 8
DAPI: 4′,6-Diamidino-2-phenylindole
EdU: 5-Ethynyl-2′-deoxyuridine
F: Forward
F4/80: F4/80 antigen
Foxp3: Forkhead box P3
G: Guanine
GAPDH: Glyceraldehyde-3-phosphate dehydrogenase
GZMB: Granzyme B
HE: Hematoxylin and eosin
Hum: Human
mRNA: Messenger RNA
Mus: Mouse
Ov-NC: Overexpression of negative control
Ov-SOX4: Overexpression of SOX4
PD-L1: Programmed cell death ligand 1
qRT-PCR: Quantitative reverse transcription-polymerase chain reaction
R: Reverse
Si-NC: Small-interfering RNA negative control
Si-SOX4: Small-interfering RNA SOX4
SOX4: SRY-box transcription factor 4
SOX4: SRY-box transcription factor 4
SR-HCC: Sorafenib-resistant hepatocellular carcinoma
SR-HepG2: Sorafenib-resistant HepG2
T: Thymine
TUNEL: Terminal deoxynucleotidyl transferase dUTP nick end labeling

AUTHOR CONTRIBUTIONS

YXJ and YLW: Conducted the research and contributed to data analysis and interpretation of the results; YXJ: Provided assistance and suggestions for the experiments. All authors participated in the drafting and critical revision of the manuscript. All authors have read and approved the final manuscript. All authors were fully involved in the work, able to take public responsibility for relevant portions of the content and agreed to be accountable for all aspects of the work, ensuring that any questions related to its accuracy or integrity are addressed. All authors meet ICMJE authorship requirements.

ETHICS APPROVAL AND CONSENT TO PARTICIPATE

The study has been approved by the Beijing Maide Kangna Laboratory Animal Welfare Ethics Committee (approval No. MDKN-2025-006) (date: 2025.02.10). This study does not involve human research, so no informed consent is required.

ACKNOWLEDGMENT

Not applicable.

FUNDING

Not applicable.

CONFLICT OF INTEREST

The authors declare no conflict of interest.

EDITORIAL/PEER REVIEW

To ensure the integrity and highest quality of CytoJournal publications, the review process of this manuscript was conducted under a **double-blind model** (authors are blinded for reviewers and vice versa) through an automatic online system.

REFERENCES

1. Wang Z, Qin H, Liu S, Sheng J, Zhang X. Precision diagnosis of hepatocellular carcinoma. Chin Med J (Engl) 2023;136:1155-65.
2. Nevola R, Ruocco R, Criscuolo L, Villani A, Alfano M, Beccia D, *et al*. Predictors of early and late hepatocellular carcinoma recurrence. World J Gastroenterol 2023;29:1243-60.
3. Meng Y, Ye F, Nie P, Zhao Q, An L, Wang W, *et al*. Immunosuppressive CD10+ ALPL+ neutrophils promote resistance to anti-PD-1 therapy in HCC by mediating irreversible exhaustion of T cells. J Hepatol 2023;79:1435-49.
4. Guo L, Hu C, Yao M, Han G. Mechanism of sorafenib resistance associated with ferroptosis in HCC. Front Pharmacol 2023;14:1207496.
5. Gao R, Kalathur RK, Coto-Llerena M, Ercan C, Buechel D, Shuang S, *et al*. YAP/TAZ and ATF4 drive resistance to sorafenib in hepatocellular carcinoma by preventing ferroptosis. EMBO Mol Med 2021;13:e14351.
6. Eun JW, Yoon JH, Ahn HR, Kim S, Kim YB, Lim SB, *et al*. Cancer-associated fibroblast-derived secreted phosphoprotein 1 contributes to resistance of hepatocellular carcinoma to sorafenib and lenvatinib. Cancer Commun (Lond) 2023;43:455-79.
7. Wang X, Hu R, Song Z, Zhao H, Pan Z, Feng Y, *et al*. Sorafenib combined with STAT3 knockdown triggers ER stress-induced HCC apoptosis and cGAS-STING-mediated anti-tumor immunity. Cancer Lett 2022;547:215880.
8. Qin Y, Han S, Yu Y, Qi D, Ran M, Yang M, *et al*. Lenvatinib in hepatocellular carcinoma: Resistance mechanisms and strategies for improved efficacy. Liver Int 2024;44:1808-31.
9. Moreno CS. SOX4: The unappreciated oncogene. Semin Cancer Biol 2020;67:57-64.
10. Bagati A, Kumar S, Jiang P, Pyrdol J, Zou AE, Godicelj A, *et al*. Integrin αvβ6-TGFβ-SOX4 pathway drives immune evasion in

triple-negative breast cancer. Cancer Cell 2021;39:54-67.e59.
11. Xu J, Ji L, Liang Y, Wan Z, Zheng W, Song X, *et al*. CircRNA-SORE mediates sorafenib resistance in hepatocellular carcinoma by stabilizing YBX1. Signal Transduct Target Ther 2020;5:298.
12. Luo X, Huang W, Li S, Sun M, Hu D, Jiang J, *et al*. SOX12 facilitates hepatocellular carcinoma progression and metastasis through promoting regulatory t-cells infiltration and immunosuppression. Adv Sci 2024;11:e2310304.
13. Xia S, Pan Y, Liang Y, Xu J, Cai X. The microenvironmental and metabolic aspects of sorafenib resistance in hepatocellular carcinoma. EBioMedicine 2020;51:102610.
14. Wang H, Li N, Liu Q, Guo J, Pan Q, Cheng B, *et al*. Antiandrogen treatment induces stromal cell reprogramming to promote castration resistance in prostate cancer. Cancer Cell 2023;41:1345-62.e9.
15. Huang Q, Xing S, Peng A, Yu Z. NORAD accelerates chemo-resistance of non-small-cell lung cancer via targeting at miR-129-1-3p/SOX4 axis. Biosci Rep 2020;40:BSR20193489.
16. Lu XJ, Gao WW, Li JC, Qin SF. miRNA-381 regulates renal cancer stem cell properties and sunitinib resistance via targeting SOX4. Biochem Biophys Rep 2023;36:101566.
17. Zhang J, Xiao C, Feng Z, Gong Y, Sun B, Li Z, *et al*. SOX4 promotes the growth and metastasis of breast cancer. Cancer Cell Int 2020;20:468.
18. Xia G, Wang A, Li L. hsa_circ_0000218/hsa-miR-139-3p/SOX4 regulatory feedback circuit influences the proliferation and apoptosis of gastric cancer cells. Cytotechnology 2022;74:89-98.
19. Zhou W, Cai C, Lu J, Fan Q. miR-129-2 upregulation induces apoptosis and promotes NSCLC chemosensitivity by targeting SOX4. Thorac Cancer 2022;13:956-64.
20. Zhang A, Miao K, Sun H, Deng CX. Tumor heterogeneity reshapes the tumor microenvironment to influence drug resistance. Int J Biol Sci 2022;18:3019-33.
21. Yang M, Li J, Gu P, Fan X. The application of nanoparticles in cancer immunotherapy: Targeting tumor microenvironment. Bioact Mater 2021;6:1973-87.
22. Liang T, Tao T, Wu K, Liu L, Xu W, Zhou D, *et al*. Cancer-associated fibroblast-induced remodeling of tumor microenvironment in recurrent bladder cancer. Adv Sci (Weinh) 2023;10:e2303230.
23. Tian X, Yan T, Liu F, Liu Q, Zhao J, Xiong H, *et al*. Link of sorafenib resistance with the tumor microenvironment in hepatocellular carcinoma: Mechanistic insights. Front Pharmacol 2022;13:991052.
24. Chen S, Du Y, Guan XY, Yan Q. The current status of tumor microenvironment and cancer stem cells in sorafenib resistance of hepatocellular carcinoma. Front Oncol 2023;13:1204513.
25. Wang Y, Wang Z, Jia F, Xu Q, Shu Z, Deng J, *et al*. CXCR4-guided liposomes regulating hypoxic and immunosuppressive microenvironment for sorafenib-resistant tumor treatment. Bioact Mater 2022;17:147-61.
26. Huang J, Yang G, Xiong X, Wang M, Yuan J, Zhang Q, *et al*. Age-related CCL12 aggravates intracerebral hemorrhage-induced brain injury via recruitment of macrophages and T lymphocytes. Aging Dis 2020;11:1103-15.
27. Li Z, Liang X, Chen X, Chen Y, Wang F, Wang S, *et al*. The role of thymus- and extrathymus-derived regulatory T cells in maternal-fetal tolerance. Front Immunol 2023;14:1109352.

How to cite this article: Jing Y, Wu Y. Sex-determining region Y-Box 4 promotes the progression of advanced hepatocellular carcinoma and enhances regulatory T-cell infiltration and immune suppression. CytoJournal. 2025;22:56. doi: 10.25259/Cytojournal_27_2025

HTML of this article is available FREE at:
https://dx.doi.org/10.25259/Cytojournal_27_2025